1128 *J. Med. Chem.* **2010,** *53,* 1128–1137
DOI: 10.1021/jm901392x

Journal of Medicinal Chemistry
Article

Pyridinylquinoxalines and Pyridinylpyridopyrazines as Lead Compounds for Novel p38α Mitogen-Activated Protein Kinase Inhibitors

Pierre Koch, Hartmut Jahns, Verena Schattel, Marcia Goettert, and Stefan Laufer*

Department of Pharmaceutical and Medicinal Chemistry, Institute of Pharmacy, Eberhard-Karls-University of Tübingen, Auf der Morgenstelle 8, 72076 Tübingen, Germany

Received September 18, 2009

Various substituted 2(3)-(4-fluorophenyl)-3(2)-(pyridin-4-yl)quinoxalines and 2(3)-(4-fluorophenyl)-3(2)-(pyridin-4-yl)pyridopyrazines were synthesized as novel p38α MAP kinase inhibitors via different short synthetic strategies with high variation possibilities. The formation of the quinoxaline/pyridopyrazine core was achieved from α-diketones and *o*-phenylenediamines/α-diaminopyridines under microwave irradiation. Introduction of an amino moiety at the pyridine C2 position of the 2(3)-(4-fluorophenyl)-3(2)-(pyridin-4-yl)quinoxalines led to compounds showing potent enzyme inhibition down to the double-digit nanomolar range (**6f**; IC_{50} = 81 nM). Replacement of the quinoxaline core with pyrido[2,3-*b*]pyrazine gave compound **9e** with superior p38α MAP kinase inhibition (IC_{50} = 38 nM).

Introduction

The p38α mitogen-activated protein (MAP)[a] kinase, a serine/threonine kinase, is a key component of the cascade leading to pro-inflammatory cytokines such as tumor necrosis factor-α and interleukin-1β.[1] This kinase is activated by infection or cellular stressors such as mechanical wear, heat, or osmotic shock.[2] Inhibition of p38α MAP kinase is therefore a promising therapeutic strategy for the treatment of cytokine-driven disorders like inflammatory bowel disease or rheumatoid arthritis. Pyridinylimidazoles like the prototype inhibitor SB203580 or the recently reported 2-alkylsulfanyl-4-(4-fluorophenyl)-5-(2-aminopyridin-4-yl)-substituted imidazoles **1** (Figure 1) are potent adenosine triphosphate (ATP) competitive p38α MAP kinase inhibitors.[3−6] The central pharmacophore of these pyridinylimidazoles consists of a vicinal 4-fluorophenyl/pyridin-4-yl system.[7] The nitrogen atom of the pyridine ring is accepting a hydrogen bond from the backbone NH group of Met109. The 4-fluorophenyl ring occupies hydrophobic region I, mainly causing selectivity.

In a continuing effort to develop improved p38α MAP kinase inhibitors, we focused our attention on the optimization of the core structure. Hence, the 4-fluorophenyl/pyridin-4-yl pharmacophore was maintained, and the five-membered imidazole core was replaced with six-membered quinoxaline and pyridopyrazine rings (Figure 1). These geometrical differences between the six- and five-membered heterocyclic cores may improve the selectivity of the quinoxaline/pyridopyrazine inhibitors toward other kinases, for example, c-Jun N-terminal kinase 3 (JNK3), as compared to the five-membered core inhibitors.[7]

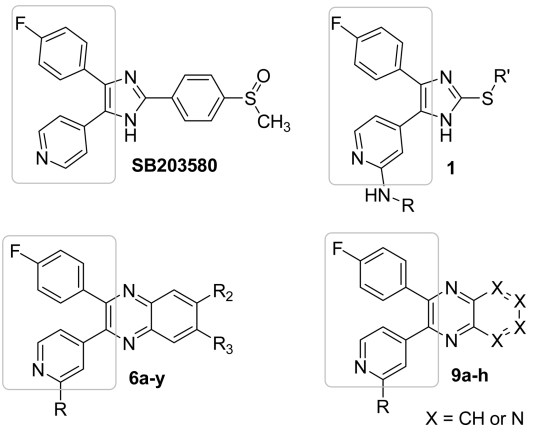

Figure 1. From five to six-membered rings. The 4-fluorophenyl/pyridin-4-yl pharmacophore is shown in a gray box.

Herein, we report different short syntheses for a series of 2(3)-aryl-3(2)-heteroarylquinoxalines **6a−y** and 2(3)-aryl-3(2)-heteroarylpyridopyrazines **9a−h** as well as their structure−activity relationships (SAR).

The main synthetic step in the preparation of the quinoxaline derivatives is the formation of heterocyclic core via click chemistry[8] starting from α-diketones and *o*-phenylenediamines. The facile introduction of substituents into the quinoxaline core is accomplished by the use of differently substituted *o*-phenylenediamines. As previously demonstrated, the reaction of α-diketones and *o*-phenylenediamines proceeded rapidly and in excellent yields when the reactants were stirred at room temperature with amidosulfonic acid (1 h),[9] iodine (3 min),[10] or cerium(IV) ammonium nitrate (10 min)[11] as a catalyst or under microwave irradiation of the reactants for 5 min in a methanol/acetic acid mixture (9:1) at 160 °C.[12] The multitude of commercially available, differently substituted *o*-phenylenediamines leads to numerous variations. The exchange of

*To whom correspondence should be addressed. Telephone: +497071-2972459. Fax: +497071-295037. E-mail: stefan.laufer@uni-tuebingen.de.

[a] Abbreviations: MAP, mitogen-activated protein; NaHMDS, sodium hexamethyldisilazane; HB, hydrogen bond; SAR, structure−activity relationship(s); JNK3, c-Jun N-terminal kinase 3; SEM, "standard error of the mean".

 Published on Web 01/15/2010

Scheme 1. Synthesis of 2-(Fluorophenyl)-3-(pyridin-4-yl)quinoxalines **6a−e**[a]

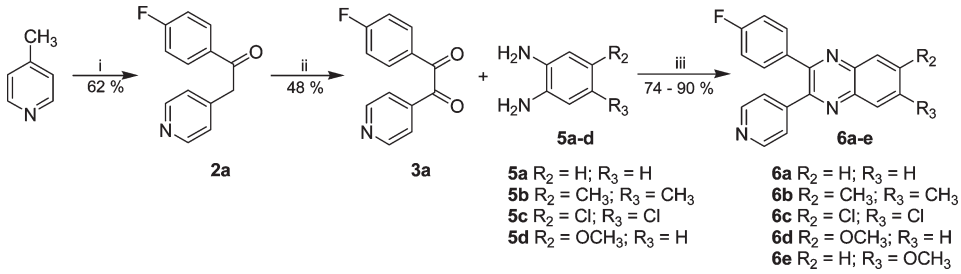

[a] Reagents and conditions: (i) NaHMDS, ethyl 4-fluorobenzoate, THF, 0 °C, 1.5 h; (ii) SeO_2, AcOH, reflux temperature, 1.5 h; (iii) MeOH/AcOH (9:1), 160 °C, 5 min, 250 W, microwave irradiation.

Scheme 2. Synthesis of 3-(2-Alkyl/phenylalkylaminopyridin-4-yl)-2-(4-fluorophenyl)quinoxalines **6f−k** (route A)[a]

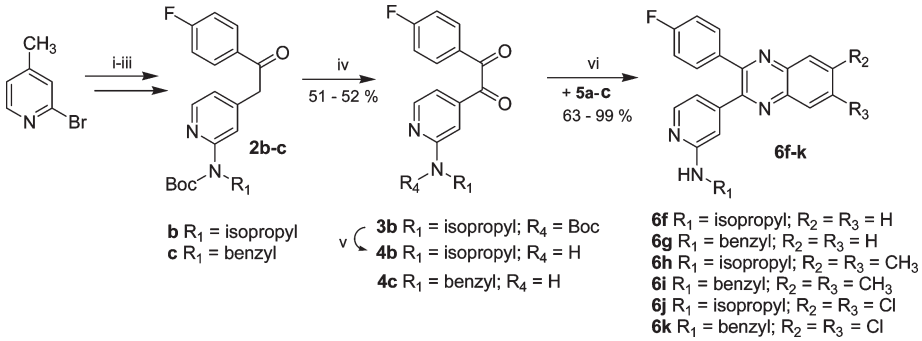

[a] Reagents and conditions: (i) R^1-NH_2, *t*BuONa, $Pd_2(dba)_3$, BINAP, toluene; (ii) Boc_2O, DMAP, DCM; (iii) NaHMDS, ethyl 4-fluorobenzoate, THF, 0 °C to rt; (iv) SeO_2, AcOH, reflux temperature, 1.5 h for **2b** and 4.5 h for **2c**; (v) TFA, DCM, rt, 16 h; (vi) MeOH/AcOH (9:1), 160 °C, 5 min, 250 W, microwave irradiation.

o-phenylenediamines in this reaction for α-diaminopyridines results in the pyridopyrazine derivatives.

Results and Discussion

Chemistry. (i) Pyridinylquinoxalines. The "unsubstituted" pyridinylquinoxaline, 2-(fluorophenyl)-3-(pyridin-4-yl)quinoxaline (Scheme 1, where R_2 and R_3 = H, **6a**), was prepared in three steps starting from 4-picoline in a straightforward synthesis (Scheme 1). 4-Picoline was deprotonated under an argon atmosphere with NaHMDS in THF at 0 °C and treated with ethyl 4-fluorobenzoate to yield 1-(4-fluorophenyl)-2-(pyridin-4-yl)ethanone (**2a**). This ethanone was oxidized with selenium dioxide in glacial acetic acid to 1-(4-fluorophenyl)-2-(pyridin-4-yl)ethane-1,2-dione (**3a**). The α-diketone **3a** and *o*-phenylenediamine (**5a**) were heated in a methanol/acetic acid mixture for 5 min at 160 °C in a microwave reactor according to the protocol of Zhao et al.[12] to yield the quinoxaline derivative **6a**.

The facile introduction of substituents (R_2 and R_3) at positions 6 and 7 of the quinoxaline core (quinoxalines **6b−e**) was accomplished by exchanging *o*-phenylenediamine with substituted *o*-phenylenediamines. Click chemistry of diketone **3a** and different substituted *o*-phenylenediamines **5a−d** led to pyridinylquinoxalines **6b−e** in good yields (Scheme 1). The reaction of the unsymmetrically substituted 4-methoxy-*o*-phenylenediamine **5d** resulted in two regioisomers, **6d** and **6e**, in a ratio of almost 1:1. These isomers were separated by flash chromatography. Slow evaporation at room temperature (rt) of a solution of the first eluted isomer **6d** in ethyl acetate resulted in crystals suitable for X-ray analysis. Compound **6d** was identified as 3-(4-fluorophenyl)-6-methoxy-2-(pyridin-4-yl)quinoxaline.[13]

Earlier analysis of the SAR of the five-membered imidazole derivatives **1** indicated that the introduction of an amino function at the pyridine C2 position resulted in another possible hydrogen bond interaction with the hinge region.[4] The introduction of this amino function was accomplished by two different synthetic methods.

The substituted 3-(2-alkyl/phenylalkylaminopyridin-4-yl)-2-(4-fluorophenyl)quinoxalines **6f−k** can be prepared via click chemistry from 1-(4-fluorophenyl)-2-[2-(alkyl/phenylalkyl)pyridin-4-yl]ethane-1,2-diones **4b** and **4c** and diverse *o*-phenylenediamine derivatives (**5a−d**) in a microwave-assisted condensation reaction in excellent yield (route A, Scheme 2). Compounds **4b** and **4c** were prepared starting from the recently published 2-{2-[boc(alkyl/phenylalkyl)amino]pyridin-4-yl}-1-(4-fluorophenyl)ethanones **2b** and **2c**[5] (Scheme 2). Ethanone **2b** was oxidized with selenium dioxide in acetic acid under reflux conditions for 1.5 h to diketone **3b** without cleavage of the boc protecting group. To remove the protecting group, diketone **3b** was treated with TFA in DCM to yield diketone **4b**. Extending the reaction time of the oxidation with selenium dioxide, for example, for compound **2c**, from 1.5 to 4.5 h permitted both the oxidation and the cleavage of the boc protecting group to compound **4c** to occur.

Finally, click chemistry of 1-(4-fluorophenyl)-2-[2-(alkyl/benzylamino)pyridin-4-yl]ethane-1,2-diones **4b** and **4c** and *o*-phenylenediamines **5a−c** led to quinoxalines **6f−k**. The limitation of route A is the introduction of the amino moiety in the first steps of the synthesis, which requires the addition and removal of a protecting group.

To overcome this drawback, we developed route B (Scheme 3) which introduced the amino function at the pyridine C2 position in the final step of the synthesis. The key intermediates for this synthetic pathway toward

Scheme 3. Synthesis of 3-(2-Alkyl/phenylalkylaminopyridin-4-yl)-2-(4-fluorophenyl)quinoxalines **6l−y** (route B)[a]

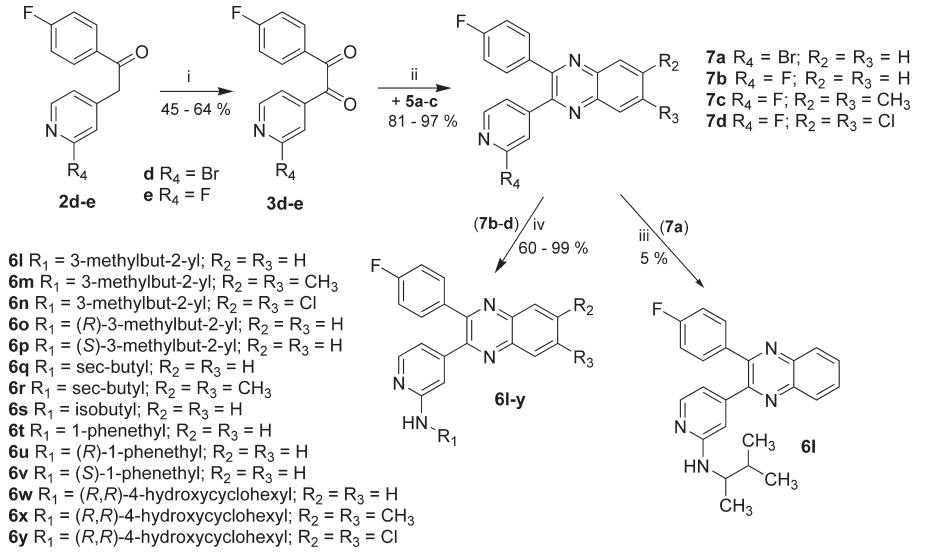

[a] Reagents and conditions: (i) SeO_2, AcOH, reflux temperature or 95 °C, 1.5 h; (ii) MeOH/AcOH (9:1), 160 °C, 5 min, 250 W, microwave irradiation; (iii) $Pd_2(dba)_3$, BINAP, *t*BuONa, 3-methylbut-2-ylamine, toluene, 120 °C, 250 W, microwave irradiation; (iv) R^1-NH_2 (excess), 160 °C, sealed glass tube (**6l−v**) or R^1-NH_2 (8 equiv), 135 °C, 1 h, 250 W, microwave irradiation (**6w−y**).

Scheme 4. Synthesis of Pyridopyrazine Derivatives **9a−h**[a]

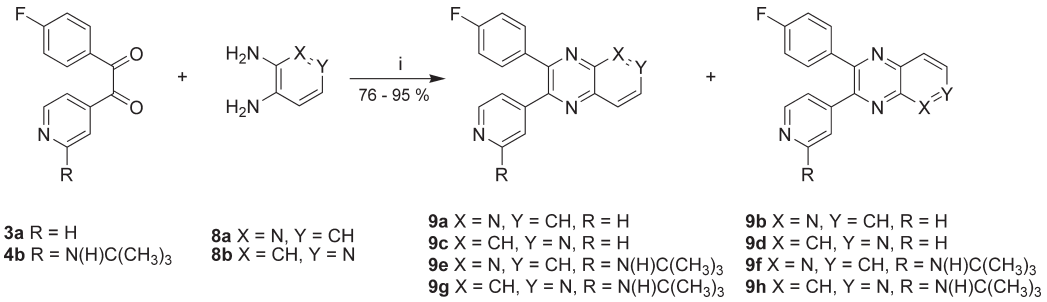

[a] Reagents and conditions: (i) MeOH/AcOH (9:1), 160 °C, 5 min, 250 W, microwave irradiation.

substituted 3-(2-alkyl/phenylalkylaminopyridin-4-yl)-2-(4-fluorophenyl)quinoxalines **6l−y** are 2-(4-fluorophenyl)-3-(halogenopyridin-4-yl)quinoxalines **7a−d** (Scheme 3), which were prepared starting from the corresponding 1-(4-fluorophenyl)-2-(2-halogenopyridin-4-yl)ethanones **2d** and **2e** followed by oxidation with selenium dioxide to diketones **3d** and **3e** followed by click chemistry with *o*-phenylenediamines **5a−c**.

The amino moiety was introduced at the pyridine C2 position via palladium-catalyzed aryl−C−N bond formation (Buchwald−Hartwig reaction) of bromo compound **7a** or via nucleophilic aromatic substitution of fluoro derivatives **7b−d**. Attempts to introduce the amino function via Buchwald−Hartwig reaction[14] under reflux conditions gave no conversion, while conducting the same reaction under microwave irradiation led to only poor yields (5%).

Hence, we endeavored to introduce the amino moieties by nucleophilic aromatic substitution (route B). In a sealed glass tube or in a microwave reactor, we heated 2-(4-fluorophenyl)-3-(2-fluoropyridin-4-yl)quinoxaline derivatives **7b−d** with an excess of the appropriate amine. After the samples had cooled to room temperature, the unreacted amine was removed and the residue was purified by flash chromatography to yield quinoxalines **6l−y** in good yields. Using route B, various substituted 3-(2-alkyl/phenylalkyl-aminopyridin-4-yl)-2-(4-fluorophenyl)quinoxalines could be prepared starting from 1-(4-fluorophenyl)-2-(2-fluoropyridin-4-yl)ethanone (**2e**) via oxidation to diketone **3e**, click chemistry to quinoxalines **7b−d**, and, finally, nucleophilic aromatic displacement of the fluoro atom with amines in three steps.

(ii) Pyridinylpyridopyrazines. Replacing the *o*-phenylenediamines with α-diaminopyridines led to pyridopyrazine derivatives **9a−h**. The two regioisomers **9a** and **9b** were obtained by reaction of diketone **3a** and 2,3-diaminopyridine (**8a**) (Scheme 4). These isomers were separated by flash chromatography and characterized by X-ray analysis.[15,16] Isomers **9c** and **9d** obtained by reaction of diketone **3a** and 3,4-diaminopyridine (**8b**) could not be separated by flash chromatography.

Click chemistry of diketone **4b**, which bears an isopropylamino moiety at the pyridine C2 position, with α-diaminopyridines **8a** and **8b** yielded pyridinylpyridopyrazines **9e−h** (Scheme 4). Isomers **9e** and **9f** could be separated by flash chromatography. Crystals suitable for X-ray analysis were obtained by slow evaporation at rt of a solution of the first eluted isomer **9e** in diethyl ether and *n*-hexane. Compound **9e** is 3-(4-fluorophenyl)-2-(2-isopropylaminopyridin-4-yl)pyrido-[2,3-*b*]pyrazine.[17] As observed for compounds **9c** and **9d** which bore no substituent at the pyridine C2 position, isomers **9g** and **9h** could not be separated by flash chromatography.

Biological Data. The inhibitory potency (as IC_{50}) of the title compounds was evaluated using a nonradioactive p38α

Table 1. Effect of Quinoxaline Core Substitution on the Biological Activity of 2(3)-(4-Fluorophenyl)-3(2)-(pyridin-4-yl)quinoxalines **6a**–**e**

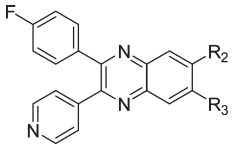

compound	R_2	R_3	IC_{50}[a] (μM) for p38α
6a	H	H	3.15 ± 0.33
6b	CH_3	CH_3	3.70 ± 0.35
6c	Cl	Cl	39% at 10 μM
6d	OCH_3	H	6.14 ± 0.77
6e	H	OCH_3	33% at 10 μM

[a] Mean values ± the standard error of the mean (SEM) of three experiments.

MAP kinase assay,[18] wherein SB203580 (IC_{50} = 0.043 ± 0.001 μM; n = 81) is used as a reference. The ability of test compounds to compete with ATP (100 μM) for the ATP binding site of the kinase correlates with the capacity of the kinase to phosphorylate ATF-2, when incubated with ATP and the test compound. Inhibition of JNK3 was assessed using a nonradioactive JNK3 assay.[19]

(i) Pyridinylquinoxalines. The effect of introducing simple substituents such as methyl, chloro, and methoxy at positions 6 and 7 of the quinoxaline core is shown in Table 1. The unsubstituted pyridinylquinoxaline, 2-(fluorophenyl)-3-(pyridin-4-yl)-quinoxaline **6a**, shows an IC_{50} value in the low micromolar range. Introduction of small substituents like a methyl group is tolerated. On the other hand, introduction of chloro (**6c**) or bulkier substituents like methoxy (**6d** and **6e**) led to inactive or less active compounds as compared to unsubstituted quinoxaline derivative **6a**.

A broad survey of amino moieties introduced at the 2 position of the pyridine ring of the pyridinylquinoxaline derivatives indicated that introduction of phenylethylamino (**6t**), aliphatic amino (**6f**, **6l**, **6q**, and **6s**), and 4-hydroxycyclohexylamino (**6w**) moieties at the pyridine C2 position increased the inhibitory potency with respect to unsubstituted compound **6a** (Table 2). Removal of the α-methyl group resulted in significantly increased IC_{50} values, and in a decline in the level of enzyme inhibition (compare **6t**–**v** vs **6g**).

We attempted to optimize the p38α MAP kinase inhibitory activity of aliphatic analogues **6f**, **6l**, **6q**, and **6s**, starting from **6l**, by the systemic, successive removal of a methyl group (Figure 2). The removal of the α-methyl group shows only a slight improvement in inhibitory activity (compare **6l** vs **6s**). Removal of the β-methyl group(s) from amino substitutents decreased the IC_{50} value from 794 nM for 3-methylbut-2-yl derivative **6l** to 114 nM for *sec*-butyl **6q**, a value that was then exceeded by that of isopropyl derivative **6f** (IC_{50} = 81 nM).

Compounds with an *S*-configuration were more potent than their counterparts with the *R*-configuration (compare **6l**, **6o**, **6p**, and **6t**–**v**). Benzylic compound **6g** was not effective (see Table 2).

Compounds listed in Table 3 have substituents both at the pyridine C2 position and at positions 6 and 7 of the quinoxaline core. For only compounds with a benzylamino moiety at the pyridine C2 position, the introduction of substituents at positions 6 and 7 led to an increased inhibitory activity. For all other compounds, the introduction of substituents at positions 6 and 7 of the heterocyclic core structure resulted in a loss of inhibitory activity.

Table 2. Biological Activity of 3(2)-(2-Alkyl/phenylalkylpyridin-4-yl)-2(3)-(4-fluorophenyl)quinoxalines **6f**, **6g**, **6l**, **6o**–**q**, and **6s**–**w** (variation of moieties at amino function R_1)

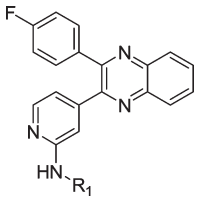

Compound	R_1	IC_{50} [μM][a] p38α
6f		0.081±0.005
6g	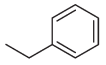	9%@10 μM
6l	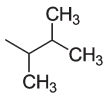	0.794±0.13
6o	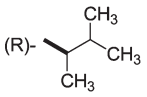	1.59±0.29
6p	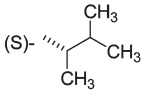	0.576±0.012
6q	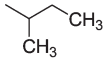	0.114±0.01
6s	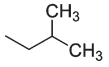	0.642±0.09
6t	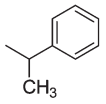	0.720±0.17
6u	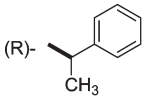	4.79±0.15
6v	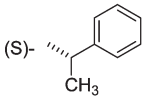	0.431±0.030
6w	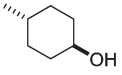	0.211±0.02

[a] Mean values ± SEM of three experiments.

The SAR of the pyridinylquinoxaline derivatives **6a**–**y** are outlined in Figure 3. The introduction of an isopropylamino moiety at the pyridine C2 position results in a 39-fold increase in inhibitory activity compared to that of unsubstituted pyridinylquinoxaline **6a**. In contrast to pyridinylimidazole derivatives **1**, substitution of the core of the pyridinylquinoxalines (R_2 and R_3) was not tolerated. For example, for compounds bearing an isopropylamino moiety at the pyridine C2 position, the introduction of two methyl

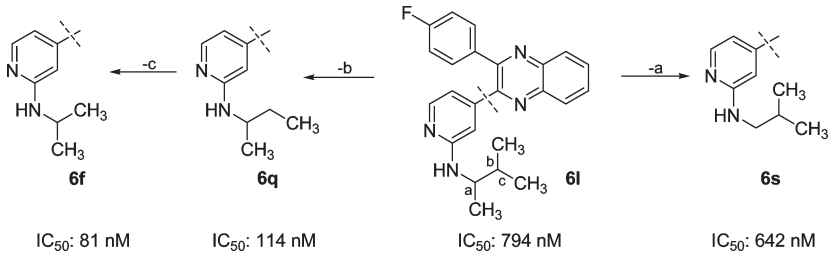

Figure 2. Compound **6l** as a starting point in the optimization of the aliphatic series.

Table 3. Biological Activity of 2(3)-(4-Fluorophenyl)-3(2)-(pyridin-4-yl)quinoxalines **6h**−**k**, **6m**, **6n**, **6r**, **6x**, and **6y** (effect of quinoxaline core substitution)

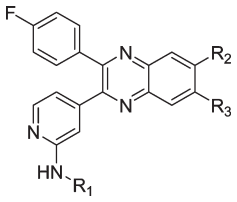

Compound	R_1	R_2	R_3	IC_{50} [μM][a] p38α
6h		-CH_3	-CH_3	0.238±0.009
6i	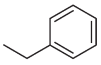	-CH_3	-CH_3	1.53±0.26
6j		-Cl	-Cl	0.412±0.028
6k	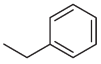	-Cl	-Cl	37%@10 μM
6m	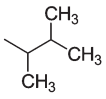	-CH_3	-CH_3	1.38±0.17
6n	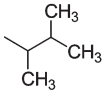	-Cl	-Cl	9.46±1.26
6r	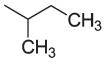	-CH_3	-CH_3	0.595±0.24
6x	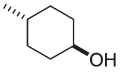	-CH_3	-CH_3	0.259±0.07
6y	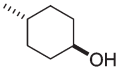	-Cl	-Cl	0.608±0.08

[a] Mean values ± SEM of three experiments.

groups or chlorine atoms at positions 6 and 7 of the quinoxaline core results in a 3- or 5-fold decrease in activity, respectively (compare **6f**, **6h**, and **6j**).

The best compound of this series, **6f**, was docked into the ATP binding site of p38α MAP kinase. Possible interactions between ATP competitive inhibitor **6f** and the ATP binding site, which is located in the cleft between the N- and C-terminal domains of p38α MAP kinase, are depicted in Figure 4. The nitrogen of the pyridin-4-yl moiety and the amino function at the pyridine C2 position form crucial hydrogen bonds to the backbone NH and CO groups of

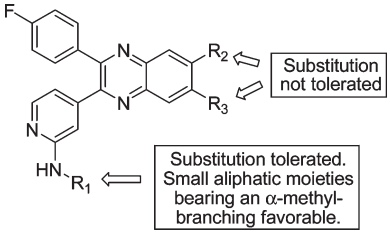

Figure 3. SAR of pyridinylquinoxaline derivatives **6**.

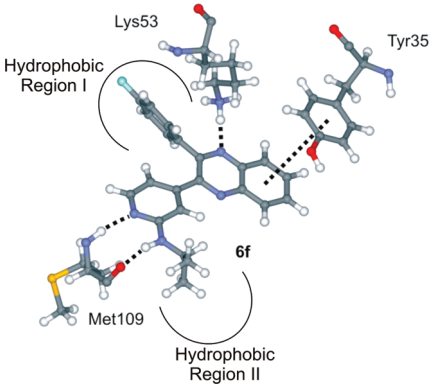

Figure 4. After geometric optimization, inhibitor **6f** was docked in the p38α active center using an induced fit docking tool.[21] As the protein model, the X-ray structure of Protein Data Bank entry 1YWR[22] was used. Possible hydrogen bonds and $\pi-\pi$ stacking interactions are shown as dashed lines.

Met109 in the hinge region. Another possible hydrogen bond interaction could be formed between N1 of the quinoxaline core and the side chain of Lys53. The 4-fluorophenyl ring binds to hydrophobic region I (selectivity pocket), which is mediated by the presence of the gatekeeper residue Thr106. The isopropyl moiety interacts with hydrophobic region II, leading to a gain in inhibitory activity. Another possible ligand−protein interaction could be a $\pi-\pi$ stacking between the aromatic side chain of Tyr35 and the phenyl system of the quinoxaline core.

(ii) Pyridinylpyridopyrazines. The biological activities of pyridinylpyridopyrazines **9a**−**d** are listed in Table 4. Compound **9a** is the only isomer of this series showing an IC_{50} value in the low micromolar range comparable to that of **6a**.

Introducing a nitrogen atom into the carbocyclic part of the quinoxaline ring can influence the atomic electrostatic potential of the nitrogen which forms a hydrogen bond (HB) to Lys53. An increase in the electrostatic potential should result in a stronger HB and in an increase in inhibitory potency.

With the Jaguar batch script hydrogen_bond.py (which is available in the Jaguar package),[20] we calculated the HB

binding energies from Lys53 to the quinoxaline and pyridopyrazine derivatives **6a**, **9a**, and **9b**. The three compounds were first docked with an induced fit docking tool[21] into the X-ray structure of Protein Data Bank entry 1YWR[22] (Figure 5). The best docking poses were used for further calculations. For the calculation of the binding energies of the hydrogen-bonded complexes, we selected the fast mode, which uses the DFT energies instead of the LMP2 energies. Additionally, all torsions were frozen during optimizations. The HB binding energies of compounds **6a**, **9a**, and **9b** are −19.15, −24.73, and −13.30 kcal/mol, respectively (Table 5). To compare the inhibitory activity of these three compounds, we calculated the quotient (Q). Q is the ratio between the IC_{50} of the reference compound of the kinase assay (SB203580) and the IC_{50} of the tested compound.

Table 4. Biological Activity of Pyridinylpyridopyrazines **9a−d**

Compound	structure	IC_{50} [μM][a] p38α
9a	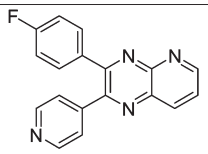	3.19±0.28
9b	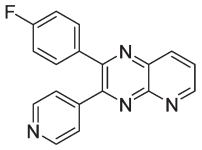	46%@10 μM
Mixture of **9c/9d**	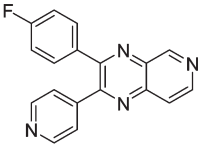 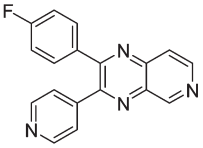	33%@10 μM

[a] Mean values ± SEM of three experiments.

3-(4-Fluorophenyl)-2-(pyridin-4-yl)pyrido[2,3-*b*]pyrazine (**9a**), having the highest quotient (Q = 0.014), also exhibited the highest HB binding energy between N4 and the ε-amino group of the Lys53 side chain of p38α MAP kinase. Conversely, **9b** with the lowest HB binding energy shows the lowest inhibitory activity (Q = 0.004).

The biological activity of pyridinylpyridopyrazines **9e−h** bearing an isopropylamino moiety at the pyridine C2 position is listed in Table 6. The SAR of compounds **9a−d** with respect to the position of the nitrogen atom of the pyridopyrazine core can be transferred to the compounds of series **9e−h**. Thus, the best compound of this series was **9e**, exhibiting an IC_{50} value in the low double-digit nanomolar range.

A comparison to quinoxaline derivative **6f** and pyridopyrazine compounds **9e** and **9f** (Figure 6) emphasizes the influence of the nitrogen atom in the carbocyclic part of the quinoxaline ring controlling the inhibitory activity. These data support the proposed hypothesis that increasing the strength of the HB to Lys53 improves the potency of the inhibitor.

Inhibition of p38α MAP Kinase versus JNK3. A comparison of inhibition of p38α MAP kinase and JNK3 for selected compounds as well as details of molecular geometry for compounds with the 4-fluorophenyl/pyridin-4-yl pharmacophore connected to five-membered (SB203580) or six-membered

Table 5. Hydrogen Bond (HB) Energies between the Heterocyclic Core and the Amino Function of the Side Chain of Lys53

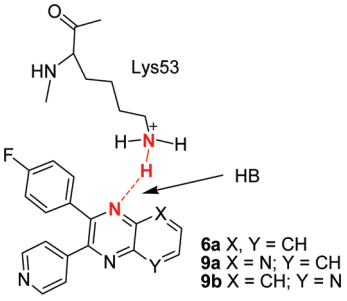

	6a	9a	9b
HB energy (kcal/mol)	−19.15	−24.73	−13.30
Q [IC_{50}(SB203580)/IC_{50}(test compound)]	0.010	0.014	0.004

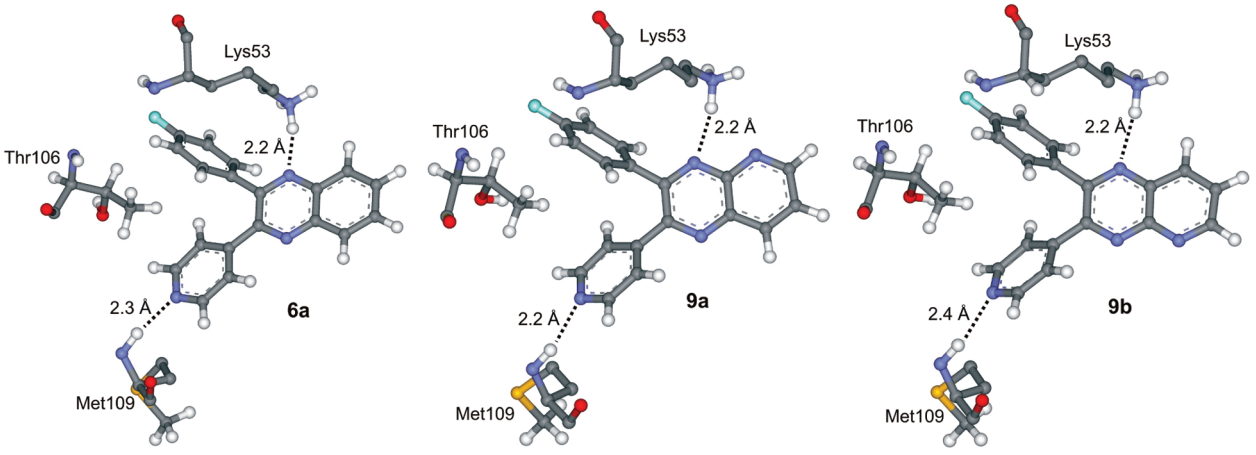

Figure 5. After geometric optimization, compounds **6a**, **9a**, and **9b** were docked in the p38α active center using an induced fit docking tool.[21] For the protein model, we used the X-ray structure of Protein Data Bank entry 1YWR.[22] Possible hydrogen bonds are shown as dashed lines, and their lengths are given.

heterocyclic core structures (quinoxaline derivatives **6a** and **6f**) is given in Table 7.

The six-membered heterocyclic quinoxaline core is fixing the 4-fluorophenyl/pyridin-4-yl pharmacophore with exocyclic bond angles between 123.3° and 125.3°. The distance between the 4-fluorophenyl and pyridin-4-yl ring (tip to tip) ranges from 7.24 to 7.36 Å. The five-membered imidazole derivative SB203580 shows larger exocyclic angles (> 131.4°) and therefore a significantly longer distance (8.28 Å) between the two aromatic rings.

The gatekeeper residue in p38α MAP kinase, Thr106, is controlling the access of the 4-fluorophenyl ring to hydrophobic region I. The more closed conformation of the 4-fluorophenyl/pyridin-4-yl pharmacophore of the six-membered ring inhibitors (quinoxalines) and the larger gatekeeper residue in JNK3 (Met146) could prevent appropriate binding access of quinoxalines to JNK3 (Figure 7). Pyridinylquinoxaline **6f** and pyridinylimidazole SB203580 have IC_{50} values for inhibition of p38α MAP kinase in the double-digit nanomolar range (Table 7). Perhaps because of these geometrical differences in the 4-fluorophenyl/pyridin-4-yl system, quinoxaline derivative **6f** shows a significant decrease in the level of inhibition of JNK3 (IC_{50} = 4 μM) compared to that of SB203580 (IC_{50} = 0.3 μM).

Table 6. Biological Activities of Isopropylamino-Substituted Pyridinylpyridopyrazines **9e**−**h**

Compound	structure	IC_{50} (μM) p38[a]
9e	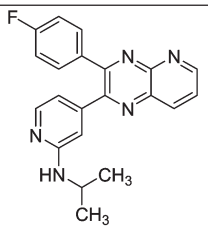	0.038±0.002
9f	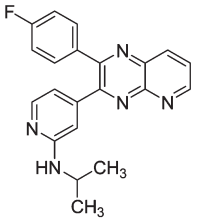	0.333±0.01
Mixture of **9g**/**9h**	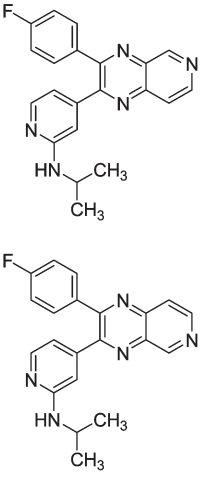	0.522±0.08

[a] Mean values ± SEM of three experiments.

Conclusion

In summary, we report short and straightforward syntheses for producing differently substituted quinoxalines **6a**−**y** and pyridopyrazines **9a**−**h** as novel p38α MAP kinase inhibitors. The various substituted 3-(2-alkyl/phenylalkylaminopyridin-4-yl)-2-(4-fluorophenyl)quinoxalines were prepared in three steps starting from ethanone **2e** (route B) via oxidation to diketone **3e**, click chemistry to quinoxalines **7b**−**d**, and nucleophilic aromatic displacement of the fluoro atom with amines.

Introduction of an amino function bearing a small aliphatic moiety at the pyridine C2 position led to another hydrogen bond to the hinge region as well as possible interaction with hydrophobic region II.

In contrast to the pyridinylimidazole SB203580 which inhibits both p38α MAP kinase and JNK3, the pyridinylquinoxalines show a clear decline in the level of inhibition of JNK3.

Introducing a nitrogen atom in the heterocyclic-free ring of the quinoxaline core influences the strength of the HB binding

Table 7. Inhibition of p38α MAP Kinase/JNK3 for Quinoxaline Derivatives **6a** and **6f** and Details of Molecular Geometry for Compounds with the 4-Fluorophenyl/pyridin-4-yl Pharmacophore Connected to Five- or Six-Membered Heterocyclic Core Structures

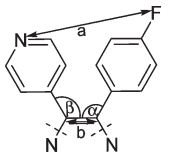

compound	IC_{50}[a] (μM) p38α	JNK3	*a* (Å)	*b* (Å)	α (deg)	β (deg)
6a	3.15 ± 0.33	31.8[c]	7.24[d]	1.39	125.2	125.3
6f	0.081 ± 0.005	3.95 ± 0.2	7.36[e]	1.43	123.3	124.3
SB203580	0.043 ± 0.001[b]	0.290 ± 0.05	8.28[f]	1.49	131.5	131.5

[a] Mean values ± SEM of three experiments. [b] Mean values ± SEM of 81 experiments. [c] Percent inhibition at 10 μM. [d] Calculated on the basis of minimization by force field. [e] See ref 17. [f] See ref 7.

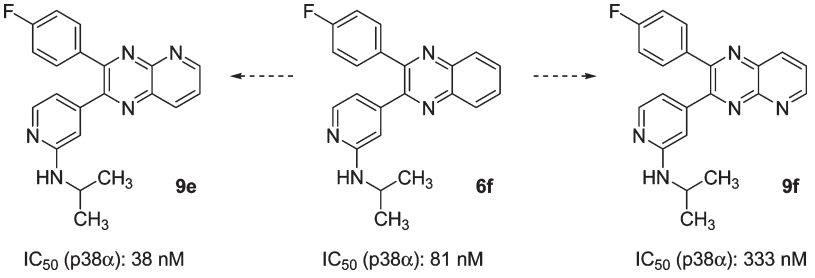

Figure 6. Comparison of compounds **6f**, **9e**, and **9f** (influence of the nitrogen atom).

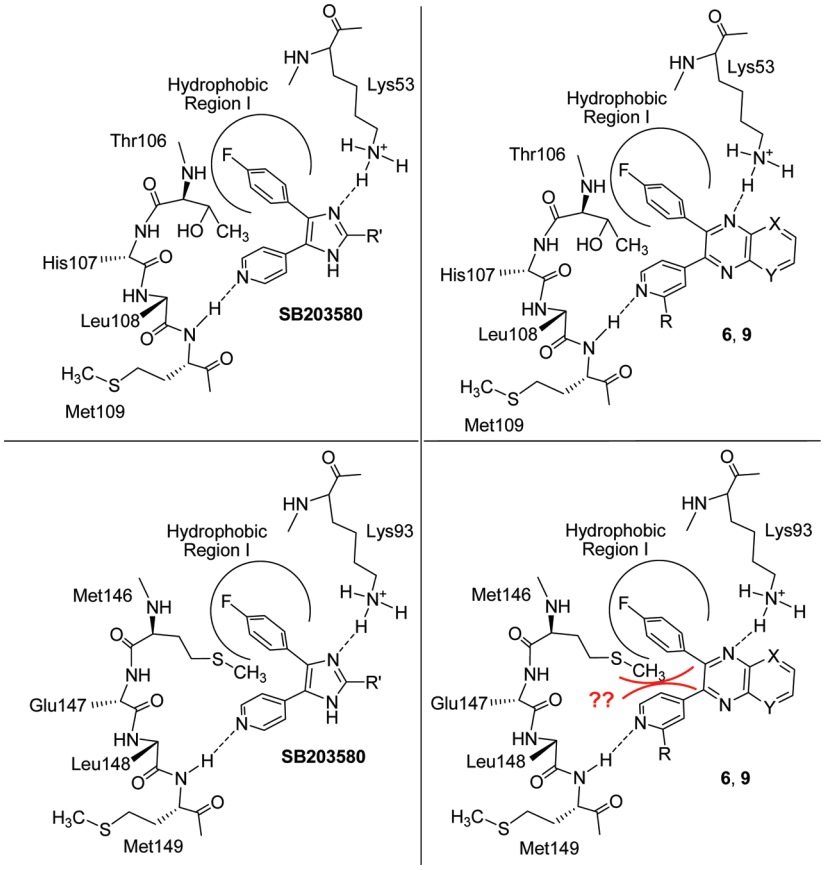

Figure 7. Comparison of possible interactions between the five-membered heterocyclic inhibitor SB203580 (left) and the six-membered heterocyclic inhibitors (right) with the binding site of p38α MAP kinase (top) and JNK3 (bottom).

energy between the heterocyclic core and the amino function of the side chain of Lys53 in the p38α MAP kinase. To this end, 3-(4-fluorophenyl)-2-(2-isopropylaminopyridin-4-yl)pyrido-[2,3-*b*]pyrazine (**9e**) was identified as the most promising kinase inhibitor.

In future attempts to prepare potent, specific kinase inhibitors, insight from our proposed binding mode may aid the design of other inhibitor structures, and the described syntheses will allow a rapid access to more pyridinylquinoxalines and -pyridopyrazines for further optimization.

Experimental Section

General. All commercially available reagents and solvents were used without further purification. The microwave reaction was performed on a CEM Discover system. NMR data were obtained on a Bruker Spectrospin AC 200 instrument at ambient temperature. High-resolution spectral mass data were obtained on a Thermo Finnigan TSQ70 instrument. The purity of the final compounds was determined by HPLC on a Hewlett-Packard HP 1090 Series II liquid chromatograph using a Betasil C8 column [150 mm × 4.6 mm (inside diameter), dp = 5 μm, (Thermo Fisher Scientific, Waltham, MA)] at 230 and 254 nm employing a gradient of 0.01 M KH_2PO_4 (pH 2.3) and methanol as the solvent system with a flow rate of 1.5 mL/min; all final compounds have a purity of >96% (see the Supporting Information for details).

General Procedure for the Preparation of Quinoxalines 6a−k via Click Chemistry (general procedure A). The α-diketone (1 equiv), *o*-phenylenediamine (1 equiv), and a methanol/glacial acetic acid mixture (9:1, v:v) were combined in a reaction vial. The reaction vessel was heated in a microwave reactor for 5 min at 160 °C (initial power of 250 W), after which a stream of compressed air cooled the reaction vessel to rt. The solvent was removed under reduced pressure, and the residue was purified by flash chromatography.

(i) 2-(4-Fluorophenyl)-3-(pyridin-4-yl)quinoxaline (6a). Compound **6a** was prepared according to general procedure A from compound **3a** (137 mg, 0.6 mmol), *o*-phenylenediamine (64 mg, 0.6 mmol), and 6 mL of a methanol/glacial acetic acid mixture (9:1). Purification: flash chromatography (SiO_2, petroleum ether/ethyl acetate, 2:1 to 1:2). Yield: 163 mg (90%), colorless solid. ^{1}H NMR (DMSO-d_6): δ 7.19−7.28 (m, 2H, C^3/C^5-H 4-F-Phe), 7.46 (dd, J_1 = 4.5 Hz, J_2 = 1.6 Hz, 2H, C^3/C^5-H Pyr), 7.51−7.58 (m, 2H, C^2/C^6-H 4-F-Phe), 7.91−7.98 (m, 2H, Quinox), 8.17−8.22 (m, 2H, Quinox), 8.60 (dd, J_1 = 4.4 Hz, J_2 = 1.6 Hz, 2H, C^2/C^6-H Pyr). EI-HRMS: calcd for $C_{19}H_{12}FN_3$ *m/z* 301.1015, observed *m/z* 301.1026.

(ii) 3-(4-Fluorophenyl)-6-methoxy-2-(pyridin-4-yl)quinoxaline (6d) and 2-(4-Fluorophenyl)-6-methoxy-3-(pyridin-4-yl)quinoxaline (6e). Compounds **6d** and **6e** were prepared according to general procedure A from compound **3a** (137 mg, 0.6 mmol), 4-methoxy-*o*-phenylenediamine (82 mg, 0.6 mmol), and 6 mL of a methanol/glacial acetic acid mixture. Purification: flash chromatography (SiO_2, petroleum ether/ethyl acetate, 2:1 to 1:2). Yield of **6d**: 82 mg (41%), colorless solid. Yield of **6e**: 73 mg (37%), colorless solid.

6d. ^{1}H NMR (DMSO-d_6): δ 3.98 (s, 3H, OCH_3), 7.18−7.27 (m, 2H, C^3/C^5-H 4-F-Phe), 7.40−7.58 (m, 6H, C^2/C^6-H 4-F-Phe, C^5/C^7-H Quinox, C^3/C^5-H Pyr), 8.04−8.09 (m, 1H, C^8-H Quinox), 8.56−8.59 (m, 2H, C^2/C^6-H Pyr). EI-HRMS: calcd for $C_{20}H_{14}FN_3O$ *m/z* 331.1120, observed *m/z* 331.1110.

The crystal structure of **6d** was determined by X-ray analysis: Enraf-Nonius CAD-4, Cu Kα, SIR92, SHELXL97. Further details of the crystal structure analysis are available in ref 13.

6e. ^{1}H NMR (DMSO-d_6): δ 3.98 (s, 3H, OCH_3), 7.18−7.23 (m, 2H, C^3/C^5-H 4-F-Phe), 7.41−7.58 (m, 6H, C^2/C^6-H

4-F-Phe, C^5/C^7-H Quinox, C^3/C^5-H Pyr), 8.05−8.10 (m, 1H, C^8-H Quinox), 8.55−8.58 (m, 2H, C^2/C^6-H Pyr). EI-HRMS: calcd for $C_{20}H_{14}FN_3O$ *m/z* 331.1120, observed *m/z* 331.1103.

(iii) 4-[3-(4-Fluorophenyl)quinoxalin-2-yl]-*N*-isopropylpyridin-2-amine (6f). Compound **6f** was prepared according to general procedure A from **4b** (44 mg, 0.15 mmol), *o*-phenylenediamine (17 mg, 0.15 mmol), and 2 mL of a methanol/glacial acetic acid mixture. Purification: flash chromatography (SiO_2, petroleum ether/ethyl acetate, 3:1 to 1:1). Yield: 55 mg (99%), colorless solid. ^{1}H NMR (DMSO-d_6): δ 1.09 (d, J = 6.4 Hz, 6H, 2× CH_3), 3.83−4.00 (m, 1H, CH), 6.35 (dd, J_1 = 5.2 Hz, J_2 = 1.2 Hz, 1H, C^5-H Pyr), 6.47 (d, J = 7.7 Hz, 1H, NH), 6.64 (s, 1H, C^3-H Pyr), 7.19−7.29 (m, 2H, C^3/C^5-H 4-F-Phe), 7.55−7.63 (m, 2H, C^2/C^6-H 4-F-Phe), 7.87−7.91 (m, 3H, C^6/C^7-H Quinox, C^6-H Pyr), 8.11−8.17 (m, 2H, C^5/C^8-H Quinox). EI-HRMS: calcd for $C_{22}H_{19}FN_4$ *m/z* 358.1594, observed *m/z* 358.1592.

The crystal structure of **6f** was determined by X-ray analysis: Enraf-Nonius CAD-4, Cu Kα, SIR92, SHELXL97. Further details of the crystal structure analysis are available in ref 17.

General Procedure for the Preparation of Quinoxalines 6l−v via Nucleophilic Aromatic Displacement (general procedure B). Compound **7b**, **7c**, or **7d** and amine compound (excess) were heated in a sealed glass tube at 160 °C. After the mixture had been cooled to rt, the amine was evaporated and the residue was purified by flash chromatography.

(i) 4-[3-(4-Fluorophenyl)quinoxalin-2-yl]-*N*-(3-methylbutan-2-yl)pyridin-2-amine (6l). Compound **6l** was prepared according to general procedure B from **7b** (76.5 mg, 0.24 mmol) and 3-methylbutan-2-amine (0.44 mL, 3.8 mmol). Reaction time: 15 h. Purification: flash chromatography (SiO_2, petroleum ether/ethyl acetate, 3:1 to 1:1). Yield: 90 mg (97%). ^{1}H NMR ($CDCl_3$): δ 0.86−0.92 (m, 6H, 2× CH_3), 1.05 (d, J = 6.6 Hz, 3H, CH_3), 1.59−1.72 (m, 1H, CH), 3.38−3.48 (m, 1H, CH), 4.59 (d, J = 8.6 Hz, 1H, NH), 6.43 (s, 1H, C^3-H Pyr), 6.65−6.69 (m, 1H, C^5-H Pyr), 7.04−7.13 (m, 2H, C^3/C^5-H 4-F-Phe), 7.55−7.62 (m, 2H, C^2/C^6-H 4-F-Phe), 7.78−7.84 (m, 2H, C^6/C^7-H Quinox), 8.07 (d, J = 5.2 Hz, 1H, C^6-H Pyr), 8.15−8.20 (m, 2H, C^5/C^8-H Quinox). EI-HRMS: calcd for $C_{24}H_{23}FN_4$ *m/z* 386.1907, observed *m/z* 386.1890.

(ii) 4-[3-(4-Fluorophenyl)quinoxalin-2-yl]-*N*-[(*R*)-3-methylbutan-2-yl]pyridin-2-amine (6o). Compound **6o** was prepared according to general procedure B from **7b** (100 mg, 0.31 mmol) and (*R*)-(−)-3-methylbutan-2-amine (1.2 mL, 10 mmol). Reaction time: 16 h. Purification: flash chromatography (SiO_2, petroleum ether/ethyl acetate, 3:1 to 1:1). Yield: 117 mg (99%). ^{1}H NMR (DMSO-d_6): δ 0.79−0.85 (m, 6H, 2× CH_3), 0.96−0.99 (m, 3H, CH_3), 1.64−1.73 (m, 1H, CH), 3.67−3.74 (m, 1H, CH), 6.34−6.45 (m, 2H, NH, C^5-H Pyr), 6.64 (s, 1H, C^3-H Pyr), 7.17−7.26 (m, 2H, C^3/C^5-H 4-F-Phe), 7.53−7.60 (m, 2H, C^2/C^6-H 4-F-Phe), 7.84−7.89 (m, 3H, C^6-H Pyr, C^6/C^7-H Quinox), 8.10−8.15 (m, 2H, C^5/C^8-H Quinox). EI-HRMS: calcd for $C_{24}H_{23}FN_4$ *m/z* 386.1907, observed *m/z* 386.1885.

(iii) 4-[3-(4-Fluorophenyl)quinoxalin-2-yl]-*N*-[(*S*)-3-methylbutan-2-yl]pyridin-2-amine (6p). Compound **6p** was prepared according to general procedure B from **7b** (100 mg, 0.31 mmol) and (*S*)-(+)-3-methylbutan-2-amine (0.56 mL, 5 mmol). Reaction time: 15 h. Purification: flash chromatography (SiO_2, petroleum ether/ethyl acetate, 3:1 to 1:1). Yield: 73 mg (60%). ^{1}H NMR (DMSO-d_6): δ 0.79−0.85 (m, 6H, 2× CH_3), 0.96−0.99 (m, 3H, CH_3), 1.64−1.73 (m, 1H, CH), 3.67−3.74 (m, 1H, CH), 6.34−6.45 (m, 2H, NH, C^5-H Pyr), 6.64 (s, 1H, C^3-H Pyr), 7.17−7.26 (m, 2H, C^3/C^5-H 4-F-Phe), 7.53−7.60 (m, 2H, C^2/C^6-H 4-F-Phe), 7.84−7.89 (m, 3H, C^6-H Pyr, C^6/C^7-H Quinox), 8.10−8.15 (m, 2H, C^5/C^8-H Quinox). EI-HRMS: calcd for $C_{24}H_{23}FN_4$ *m/z* 386.1907, observed *m/z* 386.1892.

(iv) *N*-*sec*-Butyl-4-[3-(4-fluorophenyl)quinoxalin-2-yl]pyridin-2-amine (6q). Compound **6q** was prepared according to general procedure B from **7b** (100 mg, 0.31 mmol) and *sec*-butylamine (0.51 mL, 5 mmol). Reaction time: 13 h. Purification: flash chromatography (SiO_2, petroleum ether/ethyl acetate, 3:1 to 1:1). Yield: 109 mg (94%). ^{1}H NMR (DMSO-d_6): δ 0.82 (t, J = 6.7 Hz, 3H, C^4H_3 *sec*-butyl), 1.04 (d, J = 5.3 Hz, 3H, C^1H_3-butylamine), 1.34−1.50 (m, 2H, C^3H_2 *sec*-butyl), 3.69−3.76 (m, 1H, C^2H *sec*-butyl), 6.35−6.40 (m, 2H, NH, C^5-H Pyr), 6.62 (s, 1H, C^3-H Pyr), 7.19−7.27 (m, 2H, C^3/C^5-H 4-F-Phe), 7.55−7.61 (m, 2H, C^2/C^3-H 4-F-Phe), 7.88−7.90 (m, 3H, C^6-H Pyr, C^6/C^7-H Quinox), 8.12−8.15 (m, 2H, C^4/C^8-H Quinox). EI-HRMS: calcd for $C_{23}H_{21}FN_4$ *m/z* 372.1750, observed *m/z* 372.1732.

(v) *N*-*sec*-Butyl-4-[3-(4-fluorophenyl)-6,7-dimethylquinoxalin-2-yl]pyridin-2-amine (6r). Compound **6r** was prepared according to general procedure B from **7c** (100 mg, 0.29 mmol) and *sec*-butylamine (0.47 mL, 4.6 mmol). Reaction time: 15 h. Purification: flash chromatography (SiO_2, petroleum ether/ethyl acetate, 3:1 to 1:1). Yield: 101 mg (87%). ^{1}H NMR (acetone-d_6): δ 0.85−0.93 (m, 3H, C^4H_3 *sec*-butyl), 1.10−1.13 (m, 3H, C^1H_3 *sec*-butyl), 1.41−1.55 (m, 2H, C^3H_2 *sec*-butyl), 2.49 (s, 6H, 2× CH_3, Quinox), 3.76−3.83 (m, 1H, C^2H *sec*-butyl), 5.58−5.62 (m, 1H, NH), 6.52−6.54 (m, 1H, C^5-H Pyr), 6.60 (s, 1H, C^3-H Pyr), 7.10−7.18 (m, 2H, C^3/C^5-H 4-F-Phe), 7.58−7.64 (m, 2H, C^2/C^3-H 4-F-Phe), 7.82 (s, 2H, C^5/C^8-H Quinox), 7.95−7.97 (m, 1H, C^6-H Pyr). EI-HRMS: calcd for $C_{25}H_{25}FN_4$ *m/z* 400.2063, observed *m/z* 400.2057.

(vi) 4-[3-(4-Fluorophenyl)quinoxalin-2-yl]-*N*-isobutylpyridin-2-amine (6s). Compound **6s** was prepared according to general procedure B from **7b** (100 mg, 0.31 mmol) and isobutylamine (0.52 mL, 5.0 mmol). Reaction time: 15 h. Purification: flash chromatography (SiO_2, petroleum ether/ethyl acetate, 3:1 to 1:1). Yield: 101 mg (87%). ^{1}H NMR (DMSO-d_6): δ 0.84 (d, J = 6.6 Hz, 6H, 2× CH_3 isobutyl), 1.66−1.72 (m, 1H, C^2H isobutyl), 2.84−3.00 (m, 2H, C^1H_2 isobutyl), 6.40−6.43 (m, 1H, NH), 6.59 (s, 1H, C^3-H Pyr), 6.64−6.70 (m, 1H, C^5-H Pyr), 7.19−7.28 (m, 2H, C^3/C^5-H 4-F-Phe), 7.54−7.61 (m, 2H, C^2/C^6-H Phe), 7.87−7.92 (m, 3H, 2× C-H Quinox, C^6-H Pyr), 8.12−8.17 (m, 2H, 2× C-H Quinox). EI-HRMS: calcd for $C_{23}H_{21}FN_4$ *m/z* 372.1750, observed *m/z* 372.1725.

General Procedure for the Preparation of Quinoxalines 6w−y via Nucleophilic Aromatic Displacement (general procedure C). Compound **7b**, **7c**, or **7d** and 4-*trans*-aminocyclohexanol (8 equiv) were combined in a reaction vial. The reaction vessel was heated in a microwave reactor for 1 h at 135 °C (initial power of 250 W), after which a stream of compressed air cooled the reaction vessel to rt. The reaction mixture was purified by flash chromatography.

(i) 4-{4-[3-(4-Fluorophenyl)quinoxalin-2-yl]pyridin-2-ylamin}-cyclohexanol (6w). Compound **6w** was prepared according to general procedure C from **7b** (167 mg, 0.52 mmol) and 4-*trans*-aminocyclohexanol (0.48 g, 4.18 mmol). Purification: flash chromatography (SiO_2, petroleum ether/ethyl acetate, 1:1 to 0:1). Yield: 180 mg (83%). ^{1}H NMR (DMSO-d_6): δ 1.11−1.23 (m, 4H, 2× CH_2 hydroxycyclohexyl), 1.79−1.83 (m, 4H, 2× CH_2 hydroxycyclohexyl), 3.40−3.58 (m, 2H, 2× CH hydroxycyclohexyl, H_2O in DMSO), 6.37−6.46 (m, 2H, NH, C^5-H Pyr), 6.59 (s, 1H, C^3-H Pyr), 7.23 (m, 2H, C^3/C^5-H 4-F-Phe), 7.54−7.61 (m, 2H, C^2/C^6-H 4-F-Phe), 7.85−7.91 (m, 3H, C^6-H Pyr, Quinox), 8.10−8.16 (m, 2H, Quinox). EI-HRMS: calcd for $C_{25}H_{23}FN_4O$ *m/z* 414.1856, observed *m/z* 414.1866.

General Procedure for the Preparation of Pyridopyrazines 9a−h via Click Chemistry (general procedure D). The α-diketone (1 equiv), the α-diaminopyridine (1 equiv), and a methanol/glacial acetic acid mixture (9:1, v:v) were combined in a reaction vial. The reaction vessel was heated in a microwave reactor for 5 min at 160 °C (initial power of 250 W), after which a stream of compressed air cooled the reaction vessel to rt. The solvent was removed under reduced pressure, and the residue was purified by flash chromatography.

(i) 3-(4-Fluorophenyl)-2-(pyridin-4-yl)pyrido[2,3-*b*]pyrazine (9a) and 2-(4-Fluorophenyl)-3-(pyridin-4-yl)pyrido[2,3-*b*]pyrazine (9b). Compounds **9a** and **9b** were prepared according to general procedure D from compound **3a** (113 mg, 0.5 mmol), 2,3-diaminopyridine (54 mg, 0.5 mmol), and 2 mL of a methanol/glacial acetic acid mixture (9:1). Isomers **9a** and **9b** were separated by

flash chromatography (SiO_2, petroleum ether/ethyl acetate, 1:4 to 0:1). Yield of **9a**: 67 mg (44%), colorless solid. Yield of **9b**: 65 mg (43%), colorless solid.

9a. ^{1}H NMR (DMSO-d_6): δ 7.00−7.08 (m, 2H, C^3/C^5-H 4-F-Phe), 7.43−7.46 (m, 2H, C^3/C^5-H Pyr), 7.57−7.63 (m, 2H, C^2/C^6-H 4-F-Phe), 7.72−7.78 (m, 1H, C^7-H pyridopyrazine), 8.48−8.53 (m, 1H, C^8-H pyridopyrazine), 8.64 (d, J = 5.7 Hz, 2H, C^2/C^6-H Pyr), 9.19−9.22 (m, 1H, C^6-H pyridopyrazine). EI-HRMS: calcd for $C_{18}H_{11}FN_4$ m/z 302.0968, observed m/z 302.0930.

The crystal structure of **9a** was determined by X-ray analysis: Enraf-Nonius CAD-4, Cu Kα, SIR92, SHELXL97. Further details of the crystal structure analysis are available in ref 15.

9b. ^{1}H NMR (DMSO-d_6): δ 7.03−7.12 (m, 2H, C^3/C^5-H 4-F-Phe), 7.49−7.56 (m, 4H, C^3/C^5-H Pyr, C^2/C^6-H 4-F-Phe), 7.73−7.80 (m, 1H, C^7-H pyridopyrazine), 8.49−8.54 (m, 1H, C^8-H pyridopyrazine), 8.61−8.64 (m, 2H, C^2/C^6-H Pyr), 9.19−9.21 (m, 1H, C^6-H pyridopyrazine). EI-HRMS: calcd for $C_{18}H_{11}FN_4$ m/z 302.0968, observed m/z 302.0984.

The crystal structure of **9b** was determined by X-ray analysis: Enraf-Nonius CAD-4, Cu Kα, SIR92, SHELXL97. Further details of the crystal structure analysis are available in ref 16.

(ii) 3-(4-Fluorophenyl)-2-(2-isopropylaminopyridin-4-yl)pyrido-[2,3-*b*]pyrazine (9e) and 2-(4-Fluorophenyl)-3-(2-isopropylamino-pyridin-4-yl)pyrido[2,3-*b*]pyrazine (9f). Compounds **9e** and **9f** were prepared according to general procedure D from compound **4b** (115 mg, 0.4 mmol), 2,3-diaminopyridine (44 mg, 0.4 mmol), and 3 mL of a methanol/glacial acetic acid mixture (9:1). Isomers **9e** and **9f** were separated by flash chromatography (SiO_2, petroleum ether/ethyl acetate, 1:1 to 1:4). Yield of **9e**: 46 mg (33%), yellow solid. Yield of **9f**: 62 mg (43%), yellow solid.

9e. ^{1}H NMR (DMSO-d_6): δ 1.16 (d, J = 6.3 Hz, 6H, 2× CH_3), 3.69−3.85 (m, 1H, CH), 4.55 (d, J = 7.8 Hz, 1H, NH), 6.51 (s, 1H, C^3 Pyr), 6.63 (d, J = 5.2 Hz, 1H, C^5 Pyr), 7.02−7.10 (m, 2H, C^3/C^5-H 4-F-Phe), 7.66−7.77 (m, 3H, C^7-H pyridopyrazine, C^2/C^6-H 4-F-Phe), 8.08 (d, J = 5.2 Hz, 1H, C^6-H Pyr), 8.49−8.54 (m, 1H, C^8-H pyridopyrazine), 9.18−9.21 (m, 1H, C^6-H pyridopyrazine). EI-HRMS: calcd for $C_{21}H_{18}FN_5$ m/z 359.1546, observed m/z 359.1529.

The crystal structure of **9e** was determined by X-ray analysis: Enraf-Nonius CAD-4, Cu Kα, SIR92, SHELXL97. Further details of the crystal structure analysis are available in ref 17.

9f. ^{1}H NMR (DMSO-d_6): δ 1.17 (d, J = 6.2 Hz, 6H, 2× CH_3), 3.70−3.86 (m, 1H, CH), 4.60 (d, J = 7.6 Hz, 1H, NH), 6.59 (d, J = 5.2 Hz, 1H, C^5 Pyr), 6.69 (s, 1H, C^3 Pyr), 7.05−7.13 (m, 2H, C^3/C^5-H 4-F-Phe), 7.58−7.64 (m, 2H, C^2/C^6-H 4-F-Phe), 7.72−7.78 (m, 1H, C^7-H pyridopyrazine), 8.00 (d, J = 5.0 Hz, 1H, C^6-H Pyr), 8.49−8.53 (m, 1H, C^8-H pyridopyrazine), 9.18−9.20 (m, 1H, C^6-H pyridopyrazine). EI-HRMS: calcd for $C_{21}H_{18}FN_5$ m/z 359.1546, observed m/z 359.1523.

Supporting Information Available: Experimental procedures and analytical data. This material is available free of charge via the Internet at http://pubs.acs.org.

References

(1) Chen, Z.; Gibson, T. B.; Robinson, F.; Silvestro, L.; Pearson, G.; Xu, B.; Wright, A.; Vanderbilt, C.; Cobb, M. H. MAP kinases. *Chem. Rev.* **2001**, *101*, 2449–2476.

(2) Kumar, S.; Boehm, J.; Lee, J. C. p38 MAP kinases: Key signalling molecules as therapeutic targets for inflammatory diseases. *Nat. Rev. Drug Discovery* **2003**, *2*, 717–726.

(3) Kaminska, B. MAPK signalling pathways as molecular targets for anti-inflammatory therapy: From molecular mechanisms to therapeutic benefits. *Biochim. Biophys. Acta* **2005**, *1754*, 253–262.

(4) Koch, P.; Baeuerlein, C.; Jank, H.; Laufer, S. Targeting the ribose and phosphate binding site of p38 mitogen-activated protein (MAP) kinase: Synthesis and biological testing of 2-alkylsulfanyl-, 4(5)-aryl-, 5(4)-heteroaryl-substituted imidazoles. *J. Med. Chem.* **2008**, *51*, 5630–5640.

(5) Laufer, S.; Koch, P. Towards the improvement of the synthesis of novel 4(5)-aryl-5(4)-heteroaryl-2-thio-substituted imidazoles and their p38 MAP kinase inhibitory activity. *Org. Biomol. Chem.* **2008**, *6*, 437–439.

(6) Wagner, G.; Laufer, S. Small molecular anti-cykotine agents. *Med. Res. Rev.* **2006**, *26*, 1–62.

(7) Peifer, C.; Kinkel, K.; Abadleh, M.; Schollmeyer, D.; Laufer, S. From five- to six-membered rings: 3,4-Diarylquinolinone as lead for novel p38MAP kinase inhibitors. *J. Med. Chem.* **2007**, *50*, 1213–1221.

(8) Kolb, H. C.; Finn, M. G.; Sharpless, K. B. Click chemistry: Diverse chemical function from a few good reactions. *Angew. Chem., Int. Ed.* **2001**, *40*, 2004–2021.

(9) Li, Z.; Li, W.; Sun, Y.; Huang, H.; Ouyang, P. Room temperature facile synthesis of quinoxalines catalyzed by amidosulfonic acid. *J. Heterocycl. Chem.* **2008**, *45*, 285–288.

(10) More, S. V.; Sastry, M. N. V.; Wang, C. C.; Yao, C. F. Molecular iodine. A powerful catalyst for the easy and efficient synthesis of quinoxalines. *Tetrahedron Lett.* **2005**, *46*, 6345–6348.

(11) More, S. V.; Sastry, M. N. V.; Yao, C. F. Cerium(IV) ammonium nitrate (CAN) as a catalyst in tap water: A simple, efficient and green approach to the synthesis of quinoxalines. *Green Chem.* **2006**, *8*, 91–95.

(12) Zhao, Z.; Wisnoski, D. D.; Wolkenberg, S. E.; Leister, W. H.; Wang, Y.; Lindsley, C. W. General microwave-assisted protocols for the expedient synthesis of quinoxalines and heterocyclic pyrazines. *Tetrahedron Lett.* **2004**, *45*, 4873–4876.

(13) Jahns, H.; Koch, P.; Schollmeyer, D.; Laufer, S. 3-(4-Fluorophenyl)-6-methoxy-2-(4-pyridyl)quinoxaline. *Acta Crystallogr.* **2009**, *E65*, o1626.

(14) Wolfe, J. P.; Wagaw, S.; Marcoux, J. F.; Buchwald, S. L. Rational development of practical catalysts for aromatic carbon-nitrogen bond formation. *Acc. Chem. Res.* **1998**, *31*, 805–818.

(15) Koch, P.; Schollmeyer, D.; Laufer, S. 3-(4-Fluorophenyl)-2-(4-pyridyl)pyrido[2,3-*b*]pyrazine. *Acta Crystallogr.* **2009**, *E65*, o2546.

(16) Koch, P.; Schollmeyer, D.; Laufer, S. 2-(4-Fluorophenyl)-3-(4-pyridyl)pyrido[2,3-*b*]pyrazine. *Acta Crystallogr.* **2009**, *E65*, o2512.

(17) Koch, P.; Schollmeyer, D.; Laufer, S. 4-[3-(4-Fluorophenyl)quinoxalin-2-yl]-N-isopropylpyridin-2-amine. *Acta Crystallogr.* **2009**, *E65*, o1344.

(18) Laufer, S.; Thuma, S.; Peifer, C.; Greim, C.; Herweh, Y.; Albrecht, A.; Dehner, F. An immunosorbent, nonradioactive p38 MAP kinase assay comparable to standard radioactive liquid-phase assays. *Anal. Biochem.* **2005**, *344*, 135–137.

(19) Peifer, C.; Luik, S.; Thuma, S.; Herweh, Y.; Laufer, S. Development and optimization of a non-radioactive JNK3 assay. *Comb. Chem. High Throughput Screening* **2006**, *9*, 613–618.

(20) *Jaguar*, version 7.5; Schroedinger, LLC: New York, 2008.

(21) Schroedinger Suite 2008, Induced Fit Docking Protocol. *Glide*, version 5.0; Schroedinger, LLC: New York, 2005.

(22) Golebiowski, A.; Townes, J. A.; Laufersweiler, M. J.; Brugel, T. A.; Clark, M. P.; Clark, C. M.; Djung, J. F.; Laughlin, S. K.; Sabat, M. P.; Bookland, R. G.; VanRens, J. C.; De, B.; Hsieh, L. C.; Janusz, M. J.; Walter, R. L.; Webster, M. E.; Mekel, M. J. The development of monocyclic pyrazolone based cytokine synthesis inhibitors. *Bioorg. Med. Chem. Lett.* **2005**, *15*, 2285–2289.